Received: 12 December 2017 | Revised: 17 March 2018 | Accepted: 3 May 2018

DOI: 10.4218/etrij.2017-0309

ORIGINAL ARTICLE

WILEY ETRI Journal

Novel graphene-based optical MEMS accelerometer dependent on intensity modulation

Mehdi Ahmadian | **Kian Jafari** | **Mohammad Javad Sharifi**

Department of Electrical Engineering, Shahid Beheshti University, Tehran, Iran.

Correspondence
Kian Jafari, Department of Electrical Engineering, Shahid Beheshti University, Tehran, Iran.
Email: K_jafari@sbu.ac.ir

This paper proposes a novel graphene-based optical microelectromechanical systems MEMS accelerometer that is dependent on the intensity modulation and optical properties of graphene. The designed sensing system includes a multilayer graphene finger, a laser diode (LD) light source, a photodiode, and integrated optical waveguides. The proposed accelerometer provides several advantages, such as negligible cross-axis sensitivity, appropriate linearity behavior in the operation range, a relatively broad measurement range, and a significantly wider bandwidth when compared with other important contributions in the literature. Furthermore, the functional characteristics of the proposed device are designed analytically, and are then confirmed using numerical methods. Based on the simulation results, the functional characteristics are as follows: a mechanical sensitivity of 1,019 nm/g, an optical sensitivity of 145.7 %/g, a resonance frequency of 15,553 Hz, a bandwidth of 7 kHz, and a measurement range of ±10 g. Owing to the obtained functional characteristics, the proposed device is suitable for several applications in which high sensitivity and wide bandwidth are required simultaneously.

KEYWORDS
accelerometer, graphene, intensity modulation, microelectromechanical systems

1 | INTRODUCTION

Over the past few years, the rapid development of highly reliable microelectromechanical systems (MEMS) devices, such as MEMS accelerometers, has resulted in their extensive use in a wide range of applications, such as the automotive industry, medical devices, and consumer electronics [1–4]. The basic principle of operation of a MEMS accelerometer is to measure the proof-mass displacement caused by the applied acceleration. Several technologies can be used to measure this displacement, such as capacitive technology [5–7], piezoelectric-based approaches [8], piezoresistive-sensing methods [9], and magnetic and optical techniques [10,11]. Each sensing technology not only provides several advantages but also suffers from some drawbacks. For instance, although the piezoelectric mechanism can provide a large measurement range, it may be sensitive to temperature and humidity changes, which is not suitable for MEMS devices that are required to operate in various environments. The piezoresistive-sensing mechanism may suffer from the same drawbacks. The capacitive sensing technology has been widely used in MEMS accelerometers owing to its simplicity in terms of design and fabrication, its appropriate stability against environmental changes, and the ease of its compensation approaches. However, capacitive MEMS accelerometers have some drawbacks, such as the effect of the existing parasitic capacitance, curling effect, low frequency range, and high sensitivity to electromagnetic interference (EMI). While all of the above-mentioned techniques may

encounter several issues, the optical sensing approach may introduce several advantages, such as greater immunity against EMI, higher thermal stability, better performance, and improved sensitivity compared to other existing sensing methods [12]. These advantages make the approach a suitable alternative for several applications where high sensitivity, wide bandwidth, and good reliability are crucial. Example applications include vibration analysis use for earthquake detection [13], railway technology, health monitoring applications [14], industrial testing, and process control in various industries as well as in the energy industry.

Recently, some contributions on optical MEMS accelerometers have been reported in the literature. With respect to the materials used in these optical MEMS accelerometers, silicon thin-film technologies have been extensively studied, and the proposed MEMS accelerometers are mostly made of silicon [15]. One of the main advantages of the use of silicon technology is the ease of its integration with electronics parts of the device. However, there are currently several emerging materials that can be used in MEMS technologies. These can make a difference in terms of the mechanical, electrical, optical, and thermal properties of the MEMS device, compared to silicon or other materials that are commonly used in the MEMS industry. One of the most promising candidates is graphene, which is a flat monolayer of carbon atoms tightly packed into a two-dimensional (2D) honeycomb lattice [16]. Graphene has attracted a lot of attention in recent years, and is expected to significantly impact several technological fields owing to the new applications enabled by its properties [17]. Graphene has the highest theoretical value of Young's modulus of the popular materials used in MEMS fabrication at 2 TPa and tensile strength at 130 GPa [18,19]. The Young's modulus of silicon is 169 GPa in the <110> direction and 130 GPa in the <100> direction, which is about 10% of that of graphene, while its tensile strength is much smaller than that of graphene [20]. Furthermore, the highest reported gauge factor (GF) for graphene is 1.8×10^4, whereas this factor is 30-40 for doped polysilicon [21]. In addition to several applications reported recently in [22,23], graphene has also been employed in MEMS owing to its unique mechanical properties [24–26]. However, optical and mechanical properties of this material have not been widely applied for optical MEMS (or micro-opto-electro-mechanical systems). This paper proposes a novel topology that is based on graphene for an optical MEMS accelerometer, which relies on the intensity modulation and the optical properties of graphene. The proposed microdevice can be used in a wide variety of applications, ranging from consumer electronics to inertial navigation. It provides several advantages, such as wide bandwidth, high sensitivity, small size, and cost-effectiveness compared to other existing works [15,27]. The rest of this paper is structured as follows: In Section 2, the operating principle of the proposed accelerometer is presented. Section 3 explains a model of the mechanical structure of the proposed sensor using a lumped spring-mass-damper system. Furthermore, this section introduces the design and analysis of the mechanical and optical structure using the finite-element analysis (FEA) method and the finite-difference time domain (FDTD) approach. In Section 4, a comparative discussion is presented based on the simulation results. Finally, Section 5 concludes the paper and provides different perspectives.

2 | OPERATING PRINCIPLE OF PROPOSED ACCELEROMETER

As illustrated in Figure 1, the proposed optical MEMS accelerometer varies with the intensity modulation and the optical properties of graphene. The working principle of the device is as follows: When an acceleration is applied along the positive *y*-axis direction, the proof mass is displaced, and thus, more space in the light path is blocked by the graphene finger (Figure 1). Because of the light

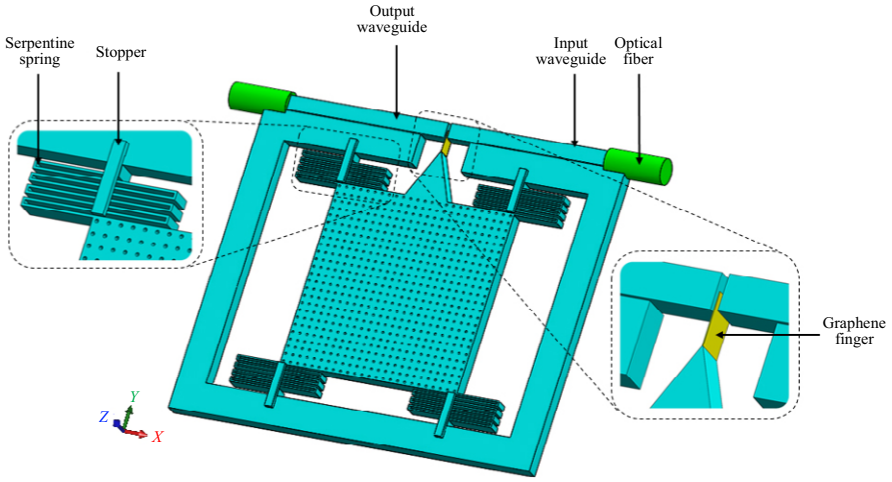

FIGURE 1 Three-dimensional structure proposed for the optical microelectromechanical systems accelerometer. The total length of the graphene finger is designed as 20 μm, and the finger is placed in the light path so that a half of its length blocks the light path, while there is no external applied acceleration

absorption of the graphene finger, the transmission is reduced and the light intensity, which is detected by the photodetector, is also reduced compared with the case in which no external acceleration is applied. This means that as a greater acceleration is applied, the larger finger length on the light path is displaced. This results in the detection of a smaller intensity by the photodetector. However, the transmission is increased while an external acceleration is applied along the negative direction of the *y*-axis under the same mechanism. Thus, the direction and magnitude of the acceleration applied to the microdevice can be determined by detecting the variation of the light intensity in the photodetector. Note that the total length of the graphene finger is set as 20 μm, and the waveguide dimensions are 20 μm × 20 μm. The light travels through the core in the fiber optic cable. The finger is placed in the light path so that one half of its length blocks the light path, while there is no external applied acceleration when the finger is placed in the light path, so half of its length blocks the light path while there is no external applied acceleration. Therefore, the proposed device can detect the applied acceleration in two directions of the *y*-axis.

3 | ANALYSIS OF THE PROPOSED ACCELEROMETER AND ITS RESULTS

3.1 | Mechanical design and analysis

The designed topology for the proposed MEMS device is illustrated in Figure 1. As shown in this figure, four serpentine springs are designed for the sensor to increase the linearity of the microdevice response. Although this type of spring may cause an increase in the cross-axis sensitivity, this factor is negligible for the proposed device owing to the designed topology. Because the applied accelerations along the *x*-axis do not change the light transmission, and to avoid the finger displacement along the *z*-axis direction, the stoppers are designed in the proposed topology (Figure 1). Structural parameters that were designed for the proposed microsensor are summarized in Table 1. Another critical functional parameter for a MEMS accelerometer is the first resonance frequency because it affects the accelerometer bandwidth and its operation. This parameter can be calculated as follows:

$$f_r = \frac{1}{2\pi}\sqrt{\frac{k_y}{m}}, \tag{1}$$

where m and k_y are the effective mass and spring constant along the sensing axis (y), respectively. As shown in Figure 2, this first resonance mode of the proposed optical MEMS device corresponding to the displacement of the proof mass along the sensing axis is 15,553 Hz, which was obtained by performing simulations using COMSOL Multiphysics. The second (f_r = 30,483 Hz) and third (f_r = 32,217 Hz) modes cause a rotational displacement of the proof mass, which may lead the device to work in undesired states. Thus, the operational bandwidth (BW) of the proposed sensor should be defined below the first resonance frequency (ie, BW = 7 kHz). As a consequence, the last three resonance modes (obtained by modal analysis of COMSOL Multiphysics) are sufficiently far from the first resonance frequency (ie, the device bandwidth) so that they do not affect the sensor operation in its operational BW. Furthermore, Figure 3 shows the frequency response of the proposed optical MEMS accelerometer. As shown in this figure, the frequency-response curve exceeds the frequency range from 0 kHz to 7 kHz. Therefore, this range can be defined as the operating BW of the proposed accelerometer, as previously mentioned.

TABLE 1 Structural parameters designed for the proposed optical microelectromechanical systems accelerometer

Parameter	Symbol	Value
Proof mass	m	2.8548275 μgr
Length × width of the proof mass	$L \times W$	250 μm × 250 μm
Thickness	t	20 μm
Length of the graphene finger	L_f	20 μm

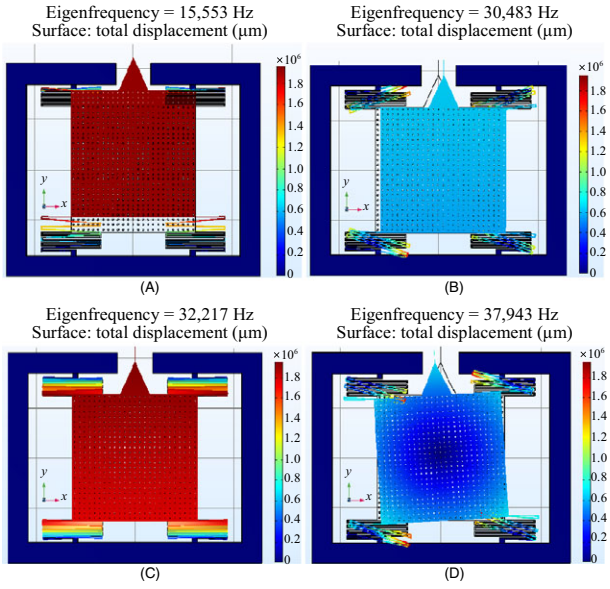

FIGURE 2 First four resonance modes of the proposed optical microelectromechanical systems accelerometer, simulated using COMSOL Multiphysics: (A) First mode (f_r = 15,553 Hz), (B) second mode (f_r = 30,483 Hz), (C) third mode (f_r = 32,217 Hz), (D) fourth mode (f_r = 37,943 Hz)

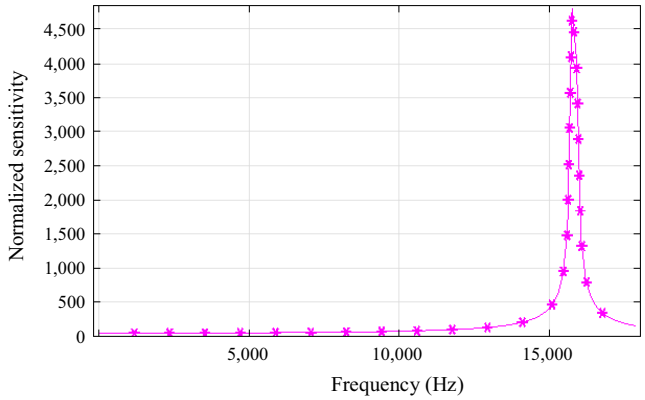

FIGURE 3 Frequency response of the proposed optical microelectromechanical systems accelerometer

Another important functional characteristic of the proposed microdevice is its mechanical sensitivity, which can be translated as the displacement of the graphene finger (and thus the changes of light transmission) with the applied acceleration. Figure 4 shows the displacement of the graphene finger for various applied accelerations based on FEA. As shown in this figure, there is a linear relationship between the displacement of the finger and the applied acceleration in the whole measurement range (the percentage of this nonlinearity is 0.7%, which can be easily neglected).

Note that the Brownian noise equivalent acceleration (BNEA) is also another characteristic of a MEMS accelerometer:

$$F = \sqrt{4K_bTR}, \tag{2}$$

where K_b is the Boltzmann constant, T is the absolute temperature, and R is the mechanical resistance, or most commonly known as a damping coefficient. However, in optical MEMS, thermal noise is the dominant noise source [28,29]. This is because thermal energy induces motion in optomechanical devices. This type of noise limits the spectral resolution or the sensitivity of the mass detectors with optical readouts. Because the thermal noise is largely dependent on the quality of the light source and that of the photodetector used for the proposed device, there is always a compromise between the final cost of the proposed device and its minimum noise density. This compromise should be made based on the target application and its desired precision.

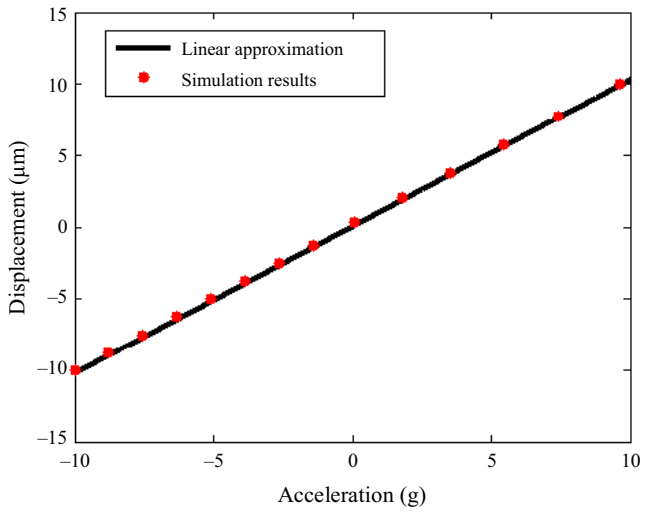

FIGURE 4 Variation in graphene finger displacement for various applied accelerations

TABLE 2 Functional characteristics of the proposed microdevice

Parameter	Analytical results	Numerical results (FEA)
Total spring constant	28.59 N/m	27.93 N/m
Mechanical sensitivity along sensing axis	1,000 nm/g	1,019 nm/g
Resonance frequency	15,742 Hz	15,553 Hz
Measurement range	±10 g	±10 g

The functional characteristics of the proposed MEMS accelerometer, which is summarized in Table 2, were obtained using an analytical approach, and were then confirmed by FEA simulations using COMSOL Multiphysics.

3.2 | Optical design and analysis

As previously mentioned in Section 1, several researchers have studied the properties of graphene in recent years [22,23,30]. This material has attracted much attention because of its exceptional properties, such as tunable bandgap [31,32], extremely high in-plane stiffness (Young's modulus), superior (highest ever measured) strength [33], high tensile strength [34], ultra-lightweight, thin nature owing to its 2D nature [17], tunable absorption, and many other factors [35,36]. In this work, we focus on graphene absorption in order to employ its properties in the proposed microdevice. It is well-known that the optical transmission is directly dependent on the optical conductance of the graphene stack for multilayer graphene, and the transmittance of graphene films as a function of the incident light frequency can be obtained by:

$$T(\omega) = \left[1 + \frac{2\pi}{c}G(\omega)\right]^{-2}, \tag{3}$$

where c and $G(\omega)$ are the speed of light and optical conductivity of the graphene film, respectively [37]. By neglecting the interlayer interaction, the optical conductivity of multilayer graphene is linearly proportional to the number of layers (N). Considering $G_1(\omega)$ as the conductivity of monolayer graphene at a frequency of ω, the above-

mentioned optical conductivity is $G(\omega) = NG_1(\omega)$. Thus, the optical transmittance of multilayer graphene can be written as [38]:

$$T(\omega) = \left[1 + \frac{2\pi}{c} NG_1(\omega)\right]^{-2}, \quad (4)$$

where $G_1(\omega) = f(\omega)G_0$, and $f(\omega)$ and G_0 are the correction coefficient and universal optical conductance, respectively. $f(\omega)$ is used to compensate the deviation between $G_1(\omega)$ and G_0. Therefore, (4) can be simplified to:

$$T(\omega) = \left[1 + f(\omega)\pi\alpha\frac{N}{2}\right]^{-2}, \quad (5)$$

where $\alpha = e^2/(\hbar c)$ is the fine-structure constant [38].

As the last step of the optical MEMS concept and prior to running the simulations on the light transmittance of the proposed microdevice, the number of graphene layers (N) used for the proposed structure (Figure 1) should be determined in order to optimize not only the performance of the proposed accelerometer, but also the device cost. In this context, the studies' results with respect to the graphene optical properties (ie, its transmittance and absorption) can help to finalize the concept of the proposed device. For instance, in [38], the authors studied the optical transmittance of multilayer graphene based on the number of graphene layers, which is summarized in Figure 5 [38].

As can be concluded from this figure, in order to increase the light absorption in the proposed device, the number of graphene layers should be increased. However, there is always a compromise between the number of layers (ie, the device performance) and the final device cost.

In addition, as seen in Figure 5, the slope of the transmittance curve decreases, while the number of graphene layers is increased. This means that increasing the number of layers by more than the threshold (ie, $20 < N < 40$) does not significantly affect the device transmittance (and thus its optical absorption). Therefore, one can choose a 20-layer graphene ($N = 20$) to design the proposed accelerometer in order to make an appropriate compromise.

After determining the number of graphene layers, the optical absorption of the graphene finger was studied for various applied accelerations, resulting in different finger displacements. Figure 6 demonstrates the results obtained using the FDTD simulations (ie, transmission vs finger displacement). Furthermore, the variation in the light transmission with the applied acceleration is illustrated in Figure 7.

Because the intensity and power of the optical source are not specified, one can calculate the changes in the transmittance of the output defect mode (T) vs the applied acceleration (a), which is the optical sensitivity of the proposed accelerometer. Note that the transmittance of the output defect mode is indicated as a percentage, which shows the ratio of the intensity of the defect mode to the intensity of the optical source. Simulation results (Figure 7) show that this optical sensitivity is $T/a = 145.7$ %/g for the proposed microdevice.

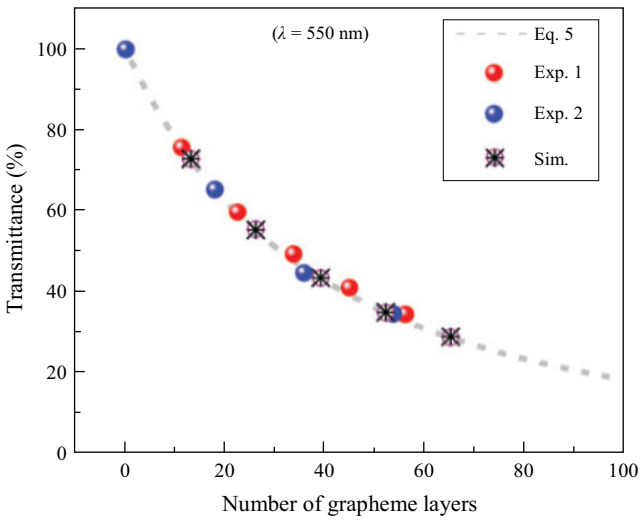

FIGURE 5 Optical transmittance of multilayer graphene based on the Kubo formula ((5) in [38]), simulation results, and measurement. The simulations were carried out in the framework of the full π-band tight-binding model. The experimental data were extracted from multistacked CVD graphene films, which were fabricated by stacking the 11.2-layer sample (red circles) and 17.8-layer sample (blue circles). The figure is reproduced from [38]

4 | DISCUSSION AND COMPARATIVE STUDY

In this section, a comparative study is carried out between the proposed graphene-based optical MEMS accelerometer

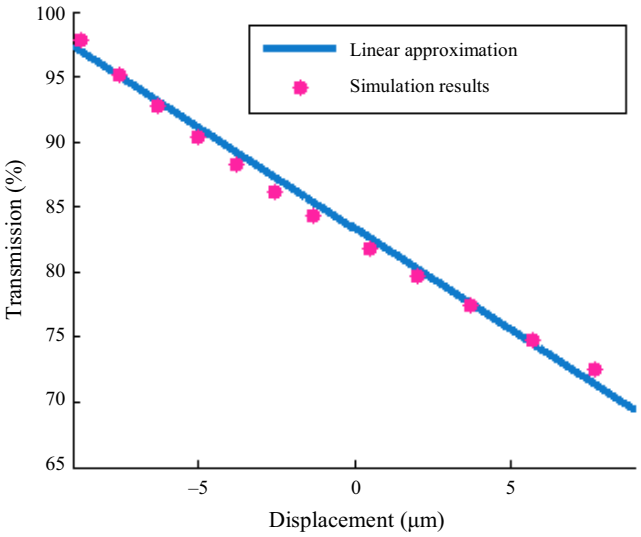

FIGURE 6 Incident light transmission vs the graphene finger displacement along the sensing direction (y)

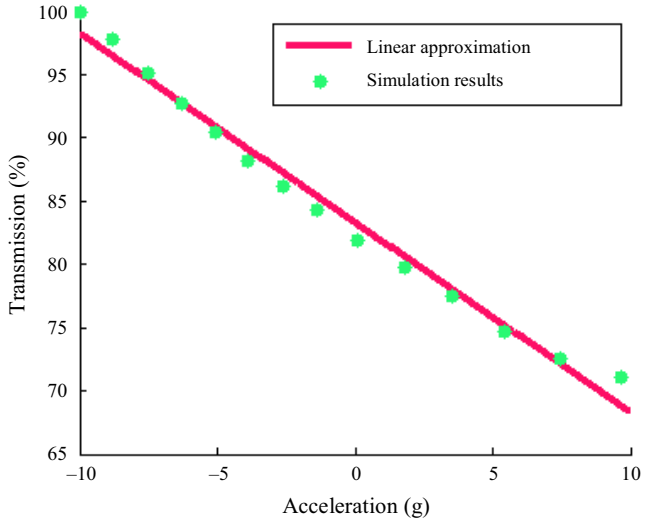

FIGURE 7 Incident light transmission vs the applied acceleration along the sensing direction (y)

and several recently developed optical MEMS accelerometers based on intensity modulation [15,27] and wavelength modulation [12].

One of the advantages of the proposed microdevice compared with the other recent works in the related domain is that it provides a wide bandwidth and a large resonance frequency, as seen in Table 3. This makes the proposed device appealing for applications in which a wide bandwidth is required, such as those mentioned in Section 1.

Another important functional characteristic for this comparative analysis is the operating measurement range. As seen in Table 3, although the proposed device has a smaller operating measurement range than in the other studies, it can provide an appropriate range for various applications such as consumer electronics, automotive, energy, medical, and other industries. Besides, the proposed graphene-based device provides not only a large mechanical sensitivity, but also a large optical sensitivity from among other sensors that depend on the intensity and wavelength modulation.

Moreover, EMI can have an undesired impact on MEMS accelerometers that depend on capacitive technology, which is the most popular sensing approach in the MEMS literature. Thus, it makes them less suitable for applications that are near strong EM fields, such as inside a generator. In addition, owing to the nature of capacitive sensing, the electronic read-out circuits have to be placed nearby, which is not suitable for use in harsh or EMI-contaminated environments. However, optical MEMS accelerometers are immune to EMI-contaminated environments because of the intrinsic immunity of the core part of the sensor against EMI as well as their capability to operate the optoelectronics circuitry remotely using optical fiber connections [15].

Because of these functional specifications, which are summarized in Table 3, the proposed graphene-based sensor provides a reliable and accurate performance over a broad range of frequencies, and can be used for various applications.

5 | CONCLUSION

This paper proposed a novel graphene-based optical MEMS accelerometer that depends on intensity modulation. FEA and FDTD simulations were performed to analyze the behavior of the proposed structure and the optical sensing system, respectively. Based on the simulation results obtained, the obtained functional characteristics of the proposed microdevice were as follows: mechanical sensitivity of 1,019 nm/g, optical sensitivity of 145.7 %/g, linear measurement range of −10 g to +10 g, first resonance frequency of 15.5 kHz, and thus a bandwidth of 7 kHz. These functional characteristics make the proposed device appealing for a wide range of applications, from consumer electronics to inertial navigation. Furthermore, the obtained functional specifications were compared with several important contributions in the related domain in order to analyze the performance of the proposed device. An ongoing work to fabricate the proposed optical MEMS accelerometer has been carried out using deep reactive-ion etching (DRIE). In addition, the built-in self-test (BIST) and built-in self-calibration of fabricated devices such as those presented in [39,40] are the focus of future works.

TABLE 3 Table showing comparison between the proposed graphene-based accelerometer and several important recent contributions in the literature

	Proposed device	**[12]**	**[15]**	**[27]**
Mechanical sensitivity $\left(\frac{\Delta x}{\Delta a}\right)$	1,019 nm/g	3.18 nm/g	60 nm/g	119.21 nm/g
Optical sensitivity $\left(\frac{\Delta T}{\Delta a}\right)$	145.7 %/g	Not reported	Not reported	0.496 %/g
Measurement range	±10 g	±22 g	±20 g	±38 g
Resonance frequency	15,553 Hz	8,908 Hz	650 Hz	1,444 Hz
Operational bandwidth	7 kHz	2 kHz	100 Hz–200 Hz	1 kHz

ACKNOWLEDGMENTS

The authors thank K. Ghasemi for the helpful discussions that were held.

ORCID


Kian Jafari http://orcid.org/0000-0003-4762-1536

REFERENCES

1. D. K. Shaeffer, *MEMS inertial sensors: A tutorial overview*, IEEE Commun. Mag. **51** (2013), no. 4, 100–109.
2. X. Zou, P. Thiruvenkatanathan, and A. A. Seshia, *A seismic-grade resonant MEMS accelerometer*, J. Microelectromechanical Syst. **23** (2014), no. 4, 768–770.
3. M. Ghanbari and M. J. Yazdanpanah, *Delay compensation of tilt sensors based on mems accelerometer using data fusion technique*, IEEE Sens. J. **15** (2015), no. 3, 1959–1966.
4. S. A. Zotov et al., *High quality factor resonant mems* accelerometer with continuous thermal compensation, IEEE Sens. J. **15** (2015), no. 9, 5045–5052.
5. M. Tsai, Y. Liu, and W. Fang, *A three-axis CMOS- MEMS accelerometer structure with vertically integrated fully differential sensing electrodes*, J. Microelectromechanical Syst. **21** (2012), no. 6, 1329–1337.
6. S. Tez et al., *A bulk-micromachined three-axis capacitive MEMS accelerometer on a single die*, J. Microelectromechanical Syst. **24** (2015), no. 5, 1264–1274.
7. V. Petkov, G. Balachandran, and J. Beintner, *A fully differential charge-balanced accelerometer for electronic stability control*, IEEE J. Solid-State Circuits **49** (2014), no. 1, 262–270.
8. N. N. Hewa-Kasakarage et al., *Micromachined piezoelectric accelerometers via epitaxial silicon cantilevers and bulk silicon proof masses*, J. Microelectromechanical Syst. **22** (2013), no. 6, 1438–1446.
9. A. Kazama, T. Aono, and R. Okada, *Stress relaxation mechanism with a ring-shaped beam for a piezoresistive three-axis accelerometer*, J. Microelectromechanical Syst. **22** (2013), no. 2, 386–394.
10. K. Zandi, J. Belanger, and Y. Peter, *Design and demonstration of an in-plane silicon-on-insulator optical MEMS Fabry Perot-based accelerometer integrated with channel waveguides*, J. Microelectromechanical Syst. **21** (2012), no. 6, 1464–1470.
11. O. Solgaard et al., *Optical MEMS: From micromirrors to complex systems*, J. Microelectromechanical Syst. **23** (2014), no. 3, 517–538.
12. A. Sheikhaleh, K. Abedi, and K. Jafari, *A proposal for an optical MEMS accelerometer relied on wavelength modulation with one dimensional photonic crystal*, J. Lightwave Technol. **34** (2016), no. 22, 5244–5249.
13. M. Kohler, T. Heaton, and M. Cheng, *The community seismic network and quake-catcher network: Enabling structural health monitoring through instrumentation by community participants*, Proc. SPIE **8692** (2013) 86923X:1–86923X:8.
14. A. Sabato et al., *A novel wireless accelerometer board for measuring low-frequency and low-amplitude structural vibration*, IEEE Sens. J. **16** (2016), no. 9, 2942–2949.
15. T. Guan et al., *MOEMS uniaxial accelerometer based on EpoClad/EpoCore photoresists with built-in fiber clamp*, Sens. Actuators A: Phys. **193** (2013), 95–102.
16. A. K. Geim and K. S. Novoselov, *The rise of graphene*, Nature Mat. **6** (2007), 183–191.
17. A. C. Ferrari et al., *Science and technology roadmap for graphene, related two-dimensional crystals, and hybrid systems*, Nanoscale **7** (2015), no. 11, 4598–4810.
18. C. Lee et al., *Measurement of the elastic properties and intrinsic strength of monolayer graphene*, Sci. **321** (2008), 385–388.
19. J. Lee, D. Yoon, and H. Cheong, *Estimation of Young's modulus of graphene by Raman spectroscopy*, Nano Lett. **12** (2012), no. 9, 4444–4448.
20. X. Zang et al., *Graphene and carbon nanotube (CNT) in MEMS/NEMS applications*, Microelectronic Eng. **132** (2015), no. C, 192–206.
21. Z. H Khan et al., *Mechanical and electromechanical properties of graphene and their potential application in MEMS*, J. Phys. D: Appl. Phys. **50** (2017), no. 5, 053003:1–053003:24.
22. F. Schwierz, *Graphene transistors*, Nature Nanotechnol. **5** (2010), no. 7, 487–496.
23. A. Krajewska et al., *Fabrication and applications of multi-layer graphene stack on transparent polymer*, Appl. Phys. Lett. **110** (2017), no. 4, 041901:1–041901:5.
24. A. D. Smith et al., *Electromechanical piezoresistive sensing in suspended graphene membranes*, Nano Lett. **13** (2013), no. 7, 3237–3242.
25. C. Martin-Olmos et al., *Graphene MEMS: AFM probe performance improvement*, ACS Nano **7** (2013), no. 5, 4164–4170.
26. W. Ren and H. Cheng, *The global growth of graphene*, Nature Nanotechnol. **9** (2014), no. 10, 726–730.
27. A. Sheikhaleh et al., *Micro-optoelectromechanical systems accelerometer based on intensity modulation using a one-dimensional photonic crystal*, Appl. Opt. **55** (2016), no. 32, 8993–8999.
28. Z. Djuric, *Mechanisms of noise sources in microelectromechanical systems*, Microelectron. Reliability **40** (2000), no. 6, 919–932.
29. F. Mohd-Yasin, D. J. Nagel, and C. E. Korman, *Noise in MEMS*, Meas. Sci. Technol. **21** (2009), no. 1, 012001:1–012001:22.
30. A. L. Hsu et al., *Graphene-based thermopile for thermal imaging applications*, Nano Lett. **15** (2015), no. 11, 7211–7216.
31. Y. Zhang et al., *Direct observation of a widely tunable bandgap in bilayer graphene*, Nature **459** (2009), 820–823.
32. C. Lui et al., *Observation of an electrically tunable band gap in trilayer graphene*, Nature Phys. **7** (2011), no. 12, 944–947.
33. I. A. Ovidko, *Mechanical properties of graphene*, Rev. Adv. Mater. Sci. **34** (2013), no. 1, 1–11.
34. Z. Xu and C. Gao, *Graphene fiber: A new trend in carbon fibers*, Mater. Today **18** (2015), no. 9, 480–492.
35. Z. Fang et al., *Active tunable absorption enhancement with graphene nanodisk arrays*, Nano Lett. **14** (2013), no. 1, 299–304.
36. S. Lee et al., *Angle-and position-insensitive electrically tunable absorption in graphene by epsilon-near-zero effect*, Opt. Express **23** (2015), no. 26, 33350–33358.
37. H. Min and A. H. MacDonald, *Origin of universal optical conductivity and optical stacking sequence identification in multilayer graphene*, Phys. Rev. Lett. **103** (2009), no. 6, 067402:1–067402:6.
38. S. Zhu, S. Yuan, and G. Janssen, *Optical transmittance of multilayer graphene*, EPL (Europhysics Lett.) **108** (2014), no. 1, 17007:1–17007:4.

39. O. Legendre et al., *A low-cost built-in self-test method for thermally actuated resistive MEMS sensors*, Sens. Actuators A: Phys. **194** (2013), 8–15.
40. K. Jafari, *A parameter estimation approach based on binary measurements using maximum likelihood analysis–Application to MEMS*, Int. J. Control Autom. Syst. **15** (2017), no. 2, 716–721.

AUTHOR BIOGRAPHIES

Mehdi Ahmadian was born in Noor, Iran. He received the BS degree in electronic engineering from Iran University of Science and Technology (IUST), Tehran, Iran, in 2015. He joined the Department of Electrical Engineering at Shahid Beheshti University, Tehran, Iran, as an exceptional talent, where he is currently working toward the MSc degree. His research focuses on the analysis, design, and modeling of nanoelectronic devices, graphene-based MEMS, and MOEMS.

Kian Jafari received his PhD in electrical engineering from SUPELEC (Paris) in 2011 with a research scholarship from the French Ministry for Higher Education and Research. His current research interests include MEMS and NEMS design and fabrication, linear and nonlinear system identification methods for different applications, such as MEMS testing.

Mohammad Javad Sharifi was born in Qom, Iran. He received the BS degree in electronic engineering from Amirkabir University of Technology (Tehran Polytechnic), Tehran, Iran, and the MS and PhD degrees from Tehran University and Amirkabir University of Technology, respectively. He is currently an associate professor with the Department of Electrical Engineering, Shahid Beheshti University, Tehran, Iran. His main research fields include nanoelectronic devices and quantum transport.